Bioelectrochemistry 75 (2009) 176–181

Contents lists available at ScienceDirect

Bioelectrochemistry

journal homepage: www.elsevier.com/locate/bioelechem

Gold nanoparticle-modified ultramicroelectrode arrays for biosensing: A comparative assessment

Jahir Orozco, Cecilia Jiménez-Jorquera, César Fernández-Sánchez *

Instituto de Microelectrónica de Barcelona (IMB-CNM), CSIC. Campus UAB, 08193 Bellaterra, Spain

ARTICLE INFO

Article history:
Received 13 January 2009
Received in revised form 23 March 2009
Accepted 29 March 2009
Available online 5 April 2009

Keywords:
Ultramicroelectrode array
Gold nanoparticles
Self-assembled monolayer
Horseradish peroxidase
Catechol

ABSTRACT

Gold ultramicroelectrode arrays (UMEAs) modified with gold nanoparticles (GNP) are shown to be a highly suitable transducer platform for the fabrication of biosensors. Comparative studies were carried out with microelectrodes and UMEAs, the latter being either bare or modified with GNPs. GNPs could be electrodeposited on to the UMEA surface, thereby increasing its active area up to one hundred times but without affecting its inherent electrodic properties. Horseradish peroxidase enzyme (HRP) was covalently immobilized over the three different transducer platforms by means of a thiol self-assembled monolayer (SAM). The resulting biosensors were applied to the amperometric detection of catechol, selected as a target analyte, at a set potential of −0.1 V vs. Ag/AgCl. The use of GNP-modified UMEAs increased the sensitivity of the developed biosensor 3-fold and 80-fold compared with the values achieved with bare UMEA and microelectrode based biosensors, respectively. The GNP-modified UMEA based biosensor showed a linear response to catechol in the concentration range from 0.1 mM to 0.4 mM, with a limit of detection of 0.05 mM.

1. Introduction

The current trend towards the miniaturisation of chemical sensors has led to the application of ultramicroelectrode arrays (UMEAs) as feasible electrochemical transducer approaches in numerous applications, including biochemical and environmental analysis [1,2]. Their advantages over conventional electrodes are widely documented [3,4]. UMEAs exhibit a greatly enhanced mass transport and very high current densities compared with conventional microelectrodes [5]. Among the different existing configurations [6] the array based on the assembly of hundreds of ultramicroelectrodes discs operating in parallel has been extensively used for the anodic stripping voltammetric detection of heavy metals [7]. However, their use for the development of biosensors has hardly been explored [8]. As observed by our group, electrodeposition of gold nanoparticles (GNP) on to a UMEA surface increases its surface area while keeping its inherent electrode features [9]. Taking advantage of this fact and based on the biocompatible microenvironment of GNP, anchorage of biorecognition elements on GNP-modified UMEA platforms could significantly improve the benefits of biosensors in terms of selectivity, sensitivity and detection limits.

Conjugation of nanoparticles with biomaterials has been intensively studied. Nanoparticles enable the electronic or optical transduction of a wide variety of biological phenomena. Moreover, the reported biocompatibility of nanoparticles may be responsible for the effective direct electron transfer between proteins and electrodes [10]. They also provide a microenvironment similar to that of the redox proteins in native systems, thus allowing immobilization of proteins without affecting their bioactivity [11,12]. In this context, GNPs have been conveniently assembled to both gold and glassy carbon electrodes for the development of biosensors [11,13,14].

Immobilization of redox enzymes on electrode surfaces for the development of bio-electrochemical sensor devices has been widely reported over the past decades [15–18]. A common methodology to immobilize biomolecules on gold metal surfaces is by means of thiolated molecules forming self-assembled monolayers (SAMs). These monolayers enable in some cases the oriented anchorage of biomolecules, thus attaining a high improvement in biosensor performance [19,20]. Nevertheless, a careful selection of the thiolated molecule has to be carried out. On one hand, SAMs formed from long thiol alkyl chains can block the electrode surface due to the formation of densely packed monolayers. On the other hand, should the thiol alkyl chains be relatively short, the surface would be just partially blocked due to the presence of defects in the SAM. Nevertheless, the electrode reaction rate can be much slower than that obtained at a bare electrode [21]. In order to improve the performance/control of the porosity of the thiolated layer, a selective desorption of the SAM can be carried out [22]. Immobilization of enzymes on nanometre-scale domains of SAMs formed with dithiobis-N-succinimidyl propionate (DTSP) and 1-tetradecanethiol [23], and with cystamine [12], have been reported.

Phenolic compounds are commonly present in nature either as a result of naturally formed products of biological degradation or by

* Corresponding author. Tel.: +34 935947700; fax: +34 935801496.
E-mail addresses: jahir.orozco@imb-cnm.csic.es (J. Orozco), cecilia.jimenez@imb-cnm.csic.es (C. Jiménez-Jorquera), cesar.fernandez@imb-cnm.csic.es (C. Fernández-Sánchez).

1567-5394/$ – see front matter © 2009 Elsevier B.V. All rights reserved.
doi:10.1016/j.bioelechem.2009.03.013

residual formation in a number of industrial processes. Thus, they are usually found as waste product in, i.e., beverages, food, mining, plastic and pharmaceutical industry. Many phenols are known to be highly toxic to man and aquatic organisms. Therefore, their measurement is of great interest. Even though there are several conventional standardised analytical methods available for the detection phenols [24,25], there is a high demand for simple and fast analyses of these kind of compounds. In this context, electrochemical laccase-based biosensors have been developed using different electrode surfaces [26–30]. Phenol determination has also been reported with other enzymatic sensors based on the use of lignin peroxidase, tyrosinase or horseradish peroxidase (HRP) [31–35]. HRP biosensor approaches appear to be sensitive to a wider range of phenolic compounds compared with tyrosinase-based ones [36].

In this work, the use of gold nanoparticles to enhance the voltammetric performance of UMEA-based biosensors is described. Using HRP as a model recognition element, a biosensor approach for the detection of the catechol phenolic compound, selected as a target analyte, was developed. The benefits of applying GNP-modified UMEAs are demonstrated by carrying out a comparative study with gold microelectrodes and bare gold UMEAs.

2. Experimental section

2.1. Reagents and solutions

Peroxidase Type II from Horseradish 181 Umg^{-1}, catechol, 20-nm gold nanoparticle stock solution containing 0.01% $HAuCl_4$ and 0.02% sodium azide, hydrogen peroxide, and dithiobis-N-succinimidyl propionate (DTSP) were purchased from Sigma-Aldrich Química S.A. (Spain). All other chemicals were of analytical grade. Solutions were prepared using 18 MΩ.cm deionised water.

2.2. Apparatus

Voltammetric experiments were performed at room temperature using a type III μ-Autolab potentiostat (Ecochemie), controlled with GPES 4.7 (General Purpose Electrochemical System) software package. Measurements were carried out with a three electrode cell consisting of a UMEA working electrode or, alternatively, a microelectrode, an on-chip counter electrode and a Ag/AgCl/10% (w/v) KNO_3 reference electrode (Metrohm 0726 100). A miniaturised Ag/AgCl pseudo-reference electrode RC6 (50-mm length, 1.5-mm external diameter from World Precision Instruments) was used for electrodeposition experiments.

2.3. Microelectrode fabrication

Au microelectrodes and Au ultramicroelectrode arrays (UMEAs) were used in this work. Both of them were fabricated at the IMB-CNM facilities with standard photolithographic techniques using Si/SiO_2/metal structures, as described elsewhere [9]. The area of microelectrodes was 1.62×10^{-2} cm^2. UMEAs with three different geometries were tested. A first array (UMEA-10) contained 100 disc-shaped microelectrodes (10 μm diameter, 100 μm interelectrode distance) having a total area of 7×10^{-5} cm^2. The second and third array contained 400 and 1600 discs, 5 μm in diameter (UMEA-5A and 5B, respectively). The interelectrode distances were 100 μm and 50 μm and the areas 7.05×10^{-5} cm^2 and 3.14×10^{-4} cm^2, respectively. Both microelectrode and UMEAs included a counter gold electrode on chip with an area of 0.7 cm^2, separated 0.5 mm from the working electrode.

2.4. Analytical approach

Microelectrodes and UMEAs were initially cleaned with 95% ethanol and acetone, followed by rinsing steps with water. A chemical cleaning process in a *Piranha* solution for 30 s was then performed in order to remove small particles coming from the UMEA fabrication and encapsulation process. Afterwards, microelectrode and UMEAs were electrochemically activated in a 0.1 M KNO_3 solution by cycling the potential from +0.8 V to −2.2 V (vs. Ag/AgCl/10% KNO_3) at a scan rate of 0.1 V s^{-1}, for at least 20 times. Cyclic voltammograms in a 0.1 M KNO_3 background solution containing 1 mM catechol were then recorded in a potential window between +0.35 V and +0.15 V, at 0.1 V s^{-1}, in order to evaluate the electrochemical surface active area and choose the suitable UMEA device geometry.

The electrodeposition of GNPs on the electrode surface was carried out as follows. Some 10 μl of the commercial GNP solution were dropped over the UMEA surface and a constant potential of +1.6 V vs. a miniaturized Ag/AgCl pseudo-reference electrode was applied for 10 min. Cyclic voltammetric scans in a potential window between −0.2 V and +1.4 V in 0.1 M H_2SO_4 /0.1 M KNO_3 at a scan rate of 0.1 V s^{-1} were carried out to estimate the microscopic surface area of the UMEAs [9].

SAMs were prepared by immersing the Au substrates in a 4 mM DTSP solution, dissolved in DMSO, for 1 h at room temperature. Then, the modified electrodes were thoroughly rinsed with DMSO and water. In order to make a characterization of the generated SAM, potential scan cycles from −0.3 V to −1.3 V were performed in a deoxygenated 0.5 M KOH solution, at a scan rate of 0.05 V s^{-1}. The SAM surface coverage (Γ) could be estimated from the areas of the different peaks recorded, which were ascribed to the reductive desorption of the adsorbed thiols, as described elsewhere [37]. The electrochemical active area of the SAM-modified electrodes was also estimated by cyclic voltammetric measurements carried out in a 0.1 M KNO_3 solution containing 1 mM catechol, in the same fashion as above.

HRP was immobilized on to the SAM-modified electrodes by immersion in 0.05 M phosphate buffer saline solution pH 7.4 (PBS), containing 10 mg ml^{-1} HRP, overnight at 4 °C. Following a washing step in PBS, the electrodes were immersed in a PBS solution containing 0.05% Tween 20 for 1 h under stirring, in order to remove any adsorbed HRP molecules from the electrode surface.

The response of the different biosensor approaches to catechol was evaluated by recording cyclic voltammograms in PBS containing 0.5 mM catechol and 0.1 mM H_2O_2. The potential was scanned between +0.35 V and −0.30 V, at a scan rate of 0.005 V s^{-1}. When not in use, the modified electrodes were stored in PBS at 4 °C.

3. Results and discussion

3.1. Voltammetric response of bare microelectrodes and UMEAs to catechol

Fig. 1 (signal 1) shows the cyclic voltammetric response of a gold microelectrode to catechol. A reversible signal related to the oxidation/reduction of the catechol/ *o*-benzoquinone species was recorded. A peak potential separation (ΔE_p) of 35 mV and cathodic to anodic peak current ratio (i_{red}/i_{ox}) of 1.1 demonstrates the reversibility of the electrochemical process at the bare gold surface and the absence of coupled chemical reactions. Fig. 2 (signal 1) shows the cyclic voltammetric response of a bare UMEA. As expected, the current recorded depended on the number, diameter and separation between adjacent ultramicroelectrode disc units of each array [9]. A limiting current plateau is not observed, which may be due to the instability of the *o*-benzoquinone species resulting from the oxidation of the catechol target analyte. It is reported that this molecule readily undergoes decomposition in aqueous solution and this process is greatly affected by the presence of catechol [38]. By contrast, a well-defined limiting current plateau was easily observed when working with other electroactive species and the same transducer platform [9].

The sensitivity to catechol, expressed as current density per concentration unit, was evaluated by chronoamperometry in a 0.1 M

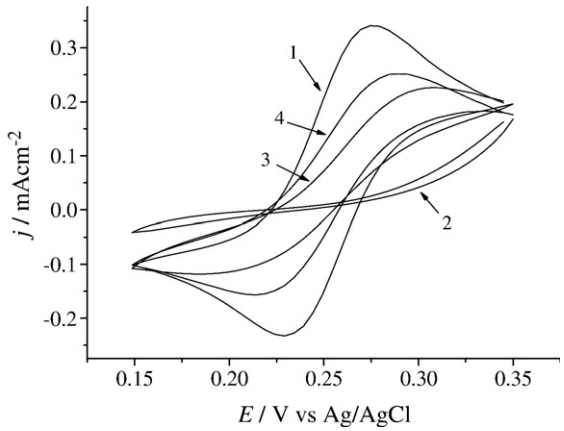

Fig. 1. Cyclic voltammetric responses recorded in a 0.1 M KNO_3 solution containing 1 mM catechol with a gold microelectrode: (1) bare; (2) coated with intact SAM; coated with SAM, (3) after thiol first selective desorption step and, (4) after thiol second selective desorption step. Scan rate: 0.1 Vs^{-1}.

KNO_3 solution containing increasing concentrations of the target analyte. The potential was set at +0.275 V and +0.310 V for the microelectrodes and the different UMEA geometries, respectively. Values are presented in Table 1. The highest sensitivity value (413.1 $\mu Acm^{-2}mM^{-1}$) was achieved with the UMEA-5A device, this being in good agreement with previous results recorded using other electroactive species [2]. Thus, this was the UMEA geometry chosen for further experiments. Previous work was carried out on the voltammetric detection of catechol using a Au electrode (1.8 mm diameter) modified with a SAM/gold nanoparticle conductive film [39]. The electrode sensitivity was 214 $\mu Acm^{-2}mM^{-1}$, which is nearly half the one obtained with the selected ultramicroelectrode array geometry.

3.2. SAM formation and selective desorption

SAMs provide one of the most elegant approaches to functionalize noble metal surfaces [40]. In this work, gold electrodes were incubated in a 4 mM DTSP solution in DMSO for 1 h. This time was long enough to get a highly blocked surface, as demonstrated by cyclic voltammetry. Indeed, the response of the resulting SAM-coated electrodes to catechol was negligible compared with that of the bare electrodes (Figs. 1 and 2, signal 2).

Voltammograms recorded in a deoxygenated 0.5 M KOH solution with SAM-coated microelectrodes show three cathodic peaks at

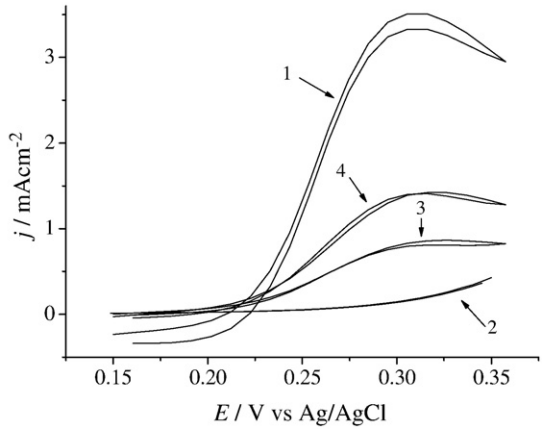

Fig. 2. Cyclic voltammetric responses recorded in a 0.1 M KNO_3 solution containing 1 mM catechol with a gold ultramicroelectrode array (UMEA-5A): (1) bare; (2) coated with intact SAM; coated with SAM, (3) after thiol first selective desorption step and, (4) after thiol second selective desorption step. Scan rate: 0.1 Vs^{-1}.

Table 1
Values of the surface area and sensitivity to catechol for the different electrode geometries.

Electrode	Area/cm^2	Sensitivity/μAcm^{-2} mM^{-1}
UMEA-10	7.85×10^{-5}	153.9
UMEA-5A	7.85×10^{-5}	413.1
UMEA-5B	3.14×10^{-4}	402.2
Microelectrode	1.62×10^{-2}	345.1

−0.6 V, −0.9 V and −1.1 V (Fig. 3, signal 1 and inset), related to the reductive desorption of the corresponding gold thiolated species from the electrode surface. A polycrystalline Au surface is considered to be formed by domains of different crystallographic orientations, also containing a high number of step edges or domain boundaries. Although a bit controversial, the presence of more than one desorption peak might be related to the thiol binding strength differences at either the exposed Au crystalline faces [41] or at Au domain and domain edges or boundaries [37]. Either way, such behaviour could be exploited in order to tailor defective SAMs, which enabled the direct electron transfer of electroactive species at the modified electrode surface. The total area of defects induced by the selective desorption of thiols could be derived from the surface coverage (Γ) of the DTSP-Au label. Γ was calculated as described in the Experimental Section and estimated to be 2.7×10^{-10} mol cm^{-2}, which corresponded to 60 ± 4% ($n=3$) of the total microelectrode area. This was calculated on the basis of the surface concentration value of a densely packed long-chain alkanethiol monolayer onto polycrystalline Au electrodes, which is 4.5×10^{-10} mol cm^{-2} [42]. Therefore, around 40% of the Au microelectrode area remained bare in the form of voids or defects after the formation of the DTSP-SAM.

In the case of SAM-coated UMEAs, three waves were also shown, at potentials similar to those recorded with the microelectrodes (Fig. 3, signal 2). The estimated Γ value was 4.49×10^{-10} mol cm^{-2}, this being around 100 ± 2% ($n=3$) of the UMEA surface. Here, thiolated molecules appeared to be more efficiently assembled and the total electrode area seemed to be coated.

Potential scans in a deoxygenated 0.5 M KOH solution were carried out for the selective desorption of the DTSP-SAM. The potential was scanned in a potential window from −0.3 V to −0.9 V, where the first two thiol desorption peaks appeared. This process was repeated twice, changing the background solution in between. After that, the presence of bare domains and/or pinholes at the Au electrode surface was checked by cyclic voltammetry. Figs. 1 and 2 (signals 3 and 4 in both figures) show the catechol voltammograms recorded with the partially unblocked Au microelectrode and UMEA surface, respectively. The characteristic anodic and cathodic signals of the catechol redox

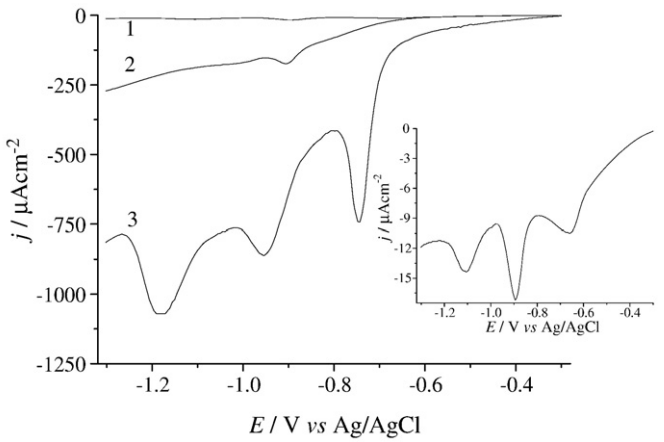

Fig. 3. Linear sweep voltammograms corresponding to the cathodic desorption of a DTSP-SAM at a (1) microelectrode, (2) a UMEA-5A, and (3) a GNP-modified UMEA-5A. Inset: amplified image of voltammogram 1. Scan rate: 0.05 Vs^{-1}.

probe were observed, which evidenced the direct electron transfer that took place at the electrode surface.

Contrary to what it was observed in this work, there is a good number of papers that deal with the application of DTSP-SAMs for the development of electrochemical biosensors on Au electrodes, where no selective desorption was carried out [43]. It is well known that short-chain organothiol molecules (number of carbon atoms ≤ 9) do not appear to completely hinder the electron transfer of electroactive species and a combined tunnelling effect and electron transfer at SAM pinholes or defects is what indeed takes place. However, in the present work, several HRP-based biosensors were fabricated using an intact DTSP SAM and no response to catechol was recorded. Similar behaviour was observed for other SAMs formed by short-chain thiolated molecules. For instance, it was previously reported that O_2 reduction was completely blocked at an intact three-carbon cysteine SAM-coated Au electrode [22]. This reaction was by contrast possible when cysteine was selectively desorbed from the electrode surface and a SAM sub-monolayer was thus obtained.

In this context, other side effects may have taken place. Short-chain SAMs appear to be selective to the size and chemical nature of the electroactive species present in solution [44]. Electrostatic repulsion could have an impact on the electron transfer process taking place at SAM modified electrodes. There are several studies of such effect reported in the literature [45]. Indeed, comparative studies carried out with charged species showed a different behaviour depending on whether both the electroactive species and the thiolated molecules possessed the same or opposite charge [46,47]. Size exclusion could also influence permeation of species across the SAM monolayer [46]. Likewise, it has been reported that chemisorbed thiol molecules adjacent to pinhole sites could be collapsed and the alkyl chain physisorbed to the gold surface, thus also inhibiting the electron transfer processes at those sites [48]. Similar effects could be taking place when working with DTSP modified gold electrodes and catechol. As shown above, selective desorption of the SAM monolayer creates well-defined voids or pinholes that greatly enhanced the catechol electron transfer at the electrode-solution interface.

3.3. GNP electrodeposition and SAM formation

The electrodeposition of gold nanoparticles on the UMEA surface increased their surface microscopic area without affecting the electrode voltammetric response, as recently reported [9]. GNPs exhibit a net negative charge induced in their preparation process. This was used to deposit them over the UMEA surface by applying a positive potential high enough to induce the discharge of the nanoparticles by anodic oxidation. During the electrodeposition process at $+1.6$ V a temporary decrease in the current was recorded. This could be explained as an oscillating electrode surface during the growth of the nanostructured gold layer. The electrodeposition was stopped when a minimum and constant current was reached, which meant that deposition of as many gold nanoparticles as possible (less than a monolayer) was guaranteed. The time and charge necessary to reach such stage was evaluated and optimized with 15 UMEAs and values were 10 min and 2.4 mC (SD = 0.2 mC) respectively. The theoretical amount of charge consumed during the reduction of a gold surface oxide monolayer (400 μC cm^{-2}) was used to calculate the GNP-modified UMEA surface microscopic area [49]. This value was compared with the experimental charge values obtained from the integration of the voltammetric signal due to gold oxide reduction, recorded in 0.1 mM H_2SO_4 solution [9]. The GNP-modified UMEA surface area was 3.50×10^{-3} cm^2, which is around 50 times larger than that of the bare UMEA but still around 5 times smaller than that of the bare microelectrode. The morphology of the gold UMEA surface before and after depositing gold nanoparticles was studied by atomic force microscopy and scanning electron microscopy techniques, as described elsewhere [2].

Cathodic desorption of DTSP SAM at GNP-modified UMEAs also gave rise to three well-defined cathodic peaks at potentials of -0.7 V, -0.9 V and -1.2 V (Fig. 3, signal 3). Such potentials were slightly more negative than those recorded with the plain UMEAs and microelectrodes. The Γ value obtained for the GNP-modified UMEAs was 1.92×10^{-10} mol cm^{-2}, which is $42 \pm 5\%$ ($n = 3$) of the electrochemical active area. In this case, over half the GNP-UMEA electrochemical surface remained bare. Here, direct electron transfer of catechol at the intact SAM-GNP-modified UMEA surface was observed, so that no selective desorption step was performed. The reason for that might be related to the high increase of the electrode surface roughness upon GNP electrodeposition [9] with a much larger number of kinks or defects. Such surface would hinder the formation of a well-ordered SAM thus leaving a higher number of surface domains

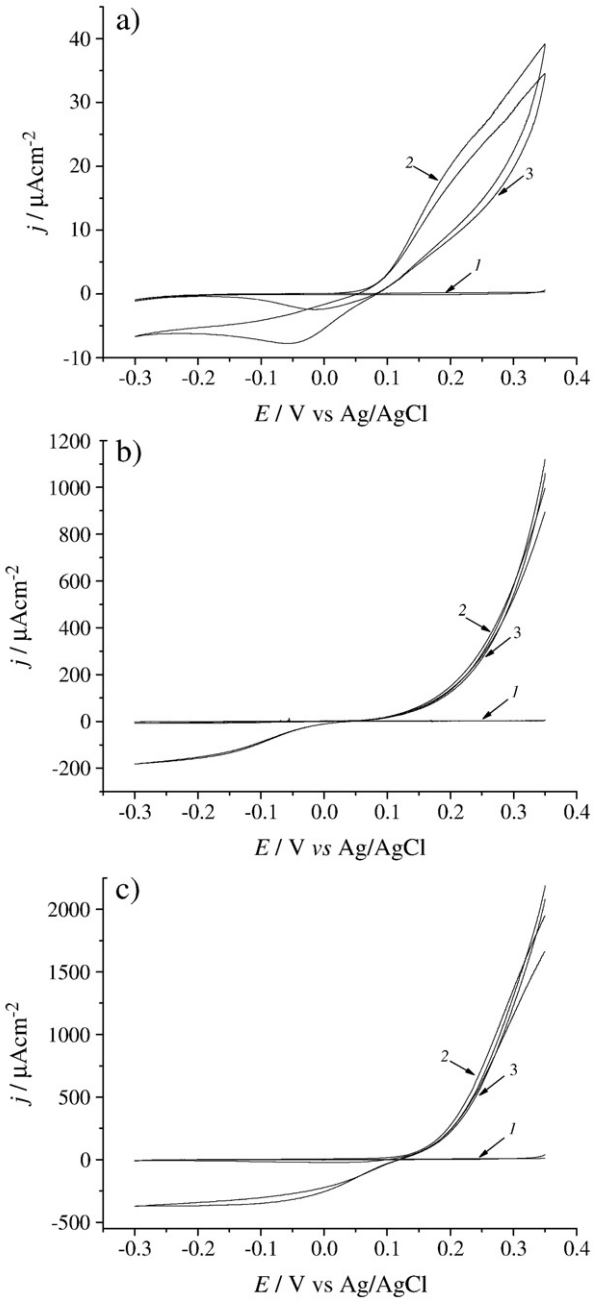

Fig. 4. Biosensor cyclic voltammetric responses of a: (a) HRP/DTSP/microelectrode; (b) a HRP/DTSP/UMEA; (c) a HRP/DTSP/GNP-modified UMEA. Signals were recorded in: (1) PBS; (2) PBS containing 0.5 mM catechol; and (3) PBS containing 0.5 mM catechol and 0.1 mM H_2O_2. Scan rate: 0.005 Vs^{-1}.

exposed. It was also reported that gold nanoparticle inherent properties make them much more reactive than gold as a bulk material [42]. This fact induces a strong interaction of the thiolated molecule with the electrodeposited GNP and may also be related to the shifting of the desorption peak potential towards more negative values, as mentioned above. In addition, it might be responsible for the enhanced electron transfer of catechol electroactive species at the SAM-GNP modified electrode.

3.4. HRP immobilisation and biosensor voltammetric characterisation

HRP was covalently attached to the modified gold surface through the formation of a peptide bond between amino moieties of its structure and the activated carboxylic group of DTSP (succinimide end-group). This procedure has being widely reported [23,43]. Cyclic voltammograms for the three prepared biosensor approaches, that is, HRP/DTSP/microelectrode, HRP/DTSP/UMEA and HRP/DTSP/GNP-modified UMEA, all of them recorded in PBS, showed that no direct electron transfer between the heme group of the HRP structure and the electrode took place (signals 1, Fig. 4). Cyclic voltammetric signals were also recorded in PBS containing 0.5 mM catechol (signals 2, Fig. 4). Anodic and cathodic faradaic currents due to the catechol electrodic process were recorded with the three different devices. When H_2O_2 was added to the catechol solution, a large cathodic current was recorded in all cases, this being related to the reduction of the *o*-benzoquinone species generated by the HRP catalytic process (signals 3, Fig. 4).

It is worth mentioning the considerable increase of the catalytic current density attained when using the HRP/DTSP/UMEA compared with that obtained with the HRP/DTSP/microelectrode (Fig. 4). Moreover, a higher increase of the catalytic current density was recorded after modification of UMEAs with nanoparticles.

3.5. Biosensor response

Catechol was chosen as a redox mediator and as a target analyte among the phenolic molecules in order to demonstrate the feasible application of this sensor approach in environmental applications. The biosensor performance is based on the catalytic reduction of the H_2O_2 to H_2O, which takes place with the concomitant oxidation of catechol to give *o*-benzoquinone. This species could be reduced back to catechol by applying a set potential of −0.1 V vs. Ag/AgCl, selected on the basis of the catalytic currents recorded and shown in Fig. 4. In this context, further experiments were conducted in PBS solutions containing 0.1 mM H_2O_2 and the biosensor response to increasing concentrations

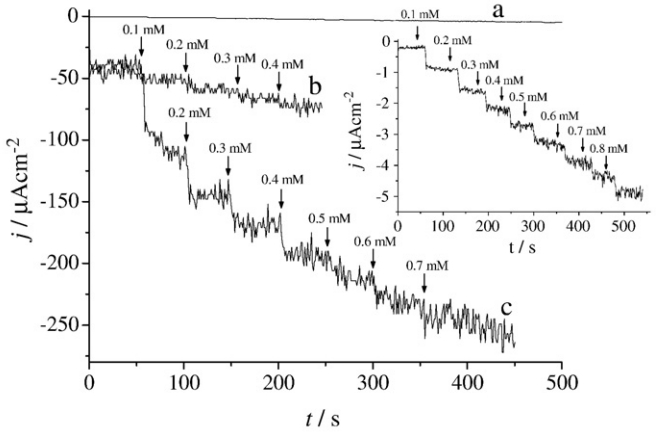

Fig. 5. Biosensor dynamic responses of a: (a) HRP/DTSP/microelectrode; (b) HRP/DTSP/UMEA; (c) HRP/DTSP/GNP-modified UMEA. Inset: amplified image of amperogram (a).

Table 2
Response characteristics of the different biosensor approaches ($n=5$, n being the number of points per calibration curve).

Electrode	Slope/µAcm^{-2} mM^{-1}	Intercept/µAcm^{-2}	r^2
HRP/DTSP/GNP-modified UMEA	228.6	71.8	0.9912
HRP/DTSP/UMEA	75.8	43.8	0.9988
HRP/DTSP/microelectrode	2.9	0.2	0.9991

of catechol was evaluated. Fig. 5 shows the dynamic response of the electrodes to additions of 0.1 mM catechol in a concentration range from 0.1 mM to 0.8 mM. An improved amperometric response was recorded with the HRP/DTSP/UMEA (Fig. 5, signal b) compared with that obtained with the HRP/DTSP/microelectrode (Fig. 5, signal a, and inset). This was the expected behaviour considering the advantageous electrodic properties of the UMEA devices. It is noteworthy the dramatic increase in the response of the HRP/DTSP/GNP-modified UMEA (Fig. 5, signal c) with respect to the other two biosensors. The values of the corresponding calibration parameters for this biosensor approach, in the linear concentration range of 0.1 mM to 0.4 mM catechol (Table 2), show a sensitivity of 228.6 µA cm^{-2}mM^{-1}. This value is around 3-fold and 80-fold higher than the values obtained with the HRP/DTSP/UMEA and the HRP/DTSP/microelectrode, respectively. The reproducibility, expressed as the RSD values obtained with three different biosensors of each configuration, was always below 10%. The repeatability was tested by means of five calibration replicates performed with a single device. Results yielded a RSD lower than 6% in all cases. The limit of detection (LOD) was calculated based on the 3Sb/m IUPAC criterion ($n=3$). For the HRP/DTSP/microelectrode the LOD was estimated in 0.015 mM catechol and for the HRP/DTSP/GNP-modified UMEA this was 0.05 mM.

As pointed out in the Introduction, there are other amperometric biosensor approaches previously reported for the detection of phenolic compounds where different enzymes were used as selective recognition elements, such as laccase, tyrosinase, HRP and lignin peroxidase [26–36]. All these works relied on the use of commercial electrodes of millimetre dimensions and different strategies for the immobilisation and detection of the target analyte. Limits of detection in the µM range were obtained in most cases. This work describes a similar approach as a proof of concept to demonstrate that such type of biosensors could be scaled down using miniaturized ultramicroelectrode arrays of planar configuration and that an enhanced performance could be attained when such transducers were modified with gold nanoparticles.

4. Conclusions

GNP-modified UMEAs are shown to be an excellent platform for the development of biosensors. The comparative study carried out with microelectrodes reveals the higher sensitivities that can be attained when working with UMEA-based devices. The simple electrodeposition process of GNP further improves the biosensor performance very highly. The benefits of this approach were demonstrated by developing a HRP biosensor for the detection of catechol, chosen as a model analyte, and bearing in mind the potential use of such platforms in the development of environmental applications. Work is in progress in order to explore the full potential of these devices in automatic systems and multiplexed approaches. Also, working with in-situ generated GNP-modified electrode surfaces and nanoparticles of other materials is being considered.

Acknowledgements

J. Orozco was supported by a research studentship from FPI Program, MEC, Spain. C. Fernández-Sánchez thanks the MICINN and CSIC for the award of a Ramon y Cajal Contract. Funding from

DEP2006-56177-CO3-02 and CSD2006-12.4615 Consolider Ingenio 2010 projects from MEC (Spain) is also acknowledged.

References

[1] M. Koudelka-Hep, P.D. van der Wal, Microelectrode sensors for biomedical and environmental applications, Electrochim. Acta 45 (2000) 2437–2441.
[2] J. Orozco, C. Fernández-Sánchez, C. Jiménez-Jorquera, Underpotential deposition-anodic stripping voltammetric detection of copper at gold nanoparticle-modified ultramicroelectrode arrays, Environ. Sci. Technol. 42 (2008) 4877–4882.
[3] K. Stulik, C. Amatore, K. Holub, V. Marecek, W. Kutner, Microelectrodes. Definitions, characterization and applications (technical report), Pure Appl. Chem. 72 (2000) 1483–1492.
[4] G. Wittstock, B. Grundig, B. Strehlitz, K. Zimmer, Evaluation of microelectrode arrays for amperometric detection by scanning electrochemical microscopy, Electroanalysis 10 (1998) 526–531.
[5] X. Xie, Assessment of a Ultramicroelectrode Array (UMEA) sensor for the determination of trace concentrations of heavy metals in water, University of Karlsruhe, Institutes für Mineralogie und Geochemie, 2004, p. 133.
[6] C. Amatore, Electrochemistry at ultramicroelectrodes, in: I. Rubistein (Ed.), Physical Electrochemistry: Principles, Methods and Applications, Marcel Dakker, New York, 1995.
[7] V. Beni, D. Arrigan, Microelectrode arrays and microfabricated devices in electrochemical stripping analysis, Curr. Anal. Chem. 4 (2008) 229–241.
[8] B. Ross, K. Cammann, Biosensor on the base of polypyrrole modified ultramicroelectrode arrays, Talanta 41 (1994) 977–983.
[9] J. Orozco, G. Suarez, C. Fernández-Sánchez, C. McNeil, C. Jiménez-Jorquera, Characterization of ultramicroelectrode arrays combining electrochemical techniques and optical microscopy imaging, Electrochim. Acta 53 (2007) 729–736.
[10] J.D. Zhang, M. Oyama, Gold nanoparticle-attached ITO as a biocompatible matrix for myoglobin immobilization: direct electrochemistry and catalysis to hydrogen peroxide, J. Electroanal. Chem. 577 (2005) 273–279.
[11] M.L. Mena, P. Yanez-Sedeno, J.M. Pingarrón, A comparison of different strategies for the construction of amperometric enzyme biosensors using gold nanoparticle-modified electrodes, Anal. Biochem. 336 (2005) 20–27.
[12] Y. Xiao, H.X. Ju, H.Y. Chen, Hydrogen peroxide sensor based on horseradish peroxidase-labeled Au colloids immobilized on gold electrode surface by cysteamine monolayer, Anal. Chim. Acta 391 (1999) 73–82.
[13] M. Li, F. Gao, P. Yang, L. Wang, B. Fang, Conveniently assembling dithiocarbamate and gold nanoparticles onto the gold electrode: a new type of electrochemical sensors for biomolecule detection, Surf. Sci. 602 (2007) 151–155.
[14] L. Zhang, X.U. Jiang, E.K. Wang, S.J. Dong, Attachment of gold nanoparticles to glassy carbon electrode and its application for the direct electrochemistry and electrocatalytic behavior of hemoglobin, Biosens. Bioelectron. 21 (2005) 337–345.
[15] I. Willner, E. Katz, Integration of layered redox proteins and conductive supports for bioelectronic applications, Angew. Chem., Int. Ed. 39 (2000) 1180–1218.
[16] Z. Cao, X. Jiang, Q. Xie, S. Yao, A third generation hydrogen peroxide biosensor based on horderadish peroxidase immobilized in a tetrathiafulvalene-tetracyanoquinodimethane/multiwalled carbon nanotubes film, Biosens. Bioelectron. 24 (2008) 222–227.
[17] X. Chen, C. Fu, Y. Wang, W. Yang, D.G. Evans, Direct electrochemisty and electrocatalysis based on a film of horseradish peroxidase intercalated into Ni–Al layered double hydroxide nanosheets, Biosens. Bioelectron. 24 (2008) 356–361.
[18] F. Wu, J. Xu, Y. Tian, Z. Hu, L. Wang, Y. Xian, L. Jin, Direct electrochemistry of horseradish peroxidase on TiO_2 nanotube arrays via seeded-grown syntesis, Biosens. Bioelectron. 24 (2008) 198–203.
[19] S.J. Choi, B.G. Choi, S.M. Park, Electrochemical sensor for electrochemically inactive beta-D(+)-glucose using alpha-cyclodextrin template molecules, Anal. Chem. 74 (2002) 1998–2002.
[20] A.G. Hansen, A. Boisen, J.U. Nielsen, H. Wackerbarth, I. Chorkendorff, J.E.T. Andersen, J.D. Zhang, J. Ulstrup, Adsorption and interfacial electron transfer of Saccharomyces cerevisiae yeast cytochrome c monolayers on Au(111) electrodes, Langmuir 19 (2003) 3419–3427.
[21] M.D. Porter, T.B. Bright, D.L. Allara, C.E.D. Chidsey, Spontaneously organized molecular assemblies. Structural characterization of normal-alkyl thiol monolayers on gold by optical ellipsometry, infrared-spectroscopy, and electrochemistry, J. Am. Chem. Soc. 109 (1987) 3559–3568.
[22] M.S. El-Deab, K. Arihara, T. Ohsaka, Fabrication of Au(111)-like polycrystalline gold electrodes and their applications to oxygen reduction, J. Elecrochem. Soc. 151 (2004) E213–E218.
[23] D. Hobara, Y. Uno, T. Kakiuchi, Immobilization of horseradish peroxidase on nanometre-scale domains of binary self-assembled monolayers formed from dithiobis-N-succinimidyl propionate and 1-tetradecanethiol on Au(111), Phys. Chem. Chem. Phys. 3 (2001) 3437–3441.
[24] F. Bosch, G. Font, J. Manes, Ultraviolet spectrophotometric determination of phenols in natural and waste-waters with iodine monobromide, Analyst 112 (1987) 1335–1337.
[25] C.P. Ong, H.K. Lee, S.F.Y. Li, Optimization of mobile phase-composition for high-performance liquid-chromatographic analysis of 11 priority substituted phenols, J. Chromatogr., A 464 (1989) 405–410.
[26] R.S. Freire, N. Duran, L.T. Kubota, Development of a laccase-based flow injection electrochemical biosensor for the determination of phenolic compounds and its application for monitoring remediation of Kraft E1 paper mill effluent, Anal Chim. Acta 463 (2002) 229–238.
[27] R.S. Freire, S. Thongngamdee, N. Duran, J. Wang, L.T. Kubota, Mixed enzyme (laccase/tyrosinase)-based remote electrochemical biosensor for monitoring phenolic compounds, Analyst 127 (2002) 258–261.
[28] J. Kulys, R. Vidziunaite, Amperometric biosensors based on recombinant laccases for phenols determination, Biosens. Bioelectron. 18 (2003) 319–325.
[29] O.D. Leite, K.O. Lupetti, O. Fatibello, I.C. Vieira, A.D. Barbosa, Synergic effect studies of the bi-enzymatic system laccase-peroxidase in a voltammetric biosensor for catecholamines, Talanta 59 (2003) 889–896.
[30] F. Vianello, A. Cambria, S. Ragusa, M.T. Cambria, L. Zennaro, A. Rigo, A high sensitivity amperometric biosensor using a monomolecular layer of laccase as biorecognition element, Biosens. Bioelectron. 20 (2004) 315–321.
[31] F. Ortega, E. Domínguez, G. Jonssonpettersson, L. Gorton, Amperometric biosensor for the determination of phenolic-compounds using a Tyrosinase graphite electrode in a flow-injection system, J. Biotechnol. 31 (1993) 289–300.
[32] T. Ruzgas, E. Csoregi, J. Emneus, L. Gorton, G. Marko-Varga, Peroxidase-modified electrodes: fundamentals and application, Anal. Chim. Acta 330 (1996) 123–138.
[33] T. Ruzgas, J. Emneus, L. Gorton, G. Marko-Varga, The development of a peroxidase biosensor for monitoring phenol and related aromatic-compounds, Anal. Chim. Acta 311 (1995) 245–253.
[34] A. Lindgren, J. Emneus, T. Ruzgas, L. Gorton, G. Marko-Varga, Amperometric detection of phenols using peroxidase-modified graphite electrodes, Anal. Chim. Acta 347 (1997) 51–62.
[35] E.E. Ferapontova, J. Castillo, L. Gorton, Bioelectrocatalytic properties of lignin peroxidase from *Phanerochaete chrysosporium* in reactions with phenols, catechols and lignin-model compounds, Biochim. Biophys. Acta (G) 1760 (2006) 1343–1354.
[36] G. Marko-Varga, J. Emneus, L. Gorton, T. Ruzgas, Development of enzyme-based amperometric sensors for the determination of phenolic-compounds, Trac-Trends Anal. Chem. 14 (1995) 319–328.
[37] L.Y.S. Lee, R.B. Lennox, Electrochemical desorption of *n*-alkylthiol SAMs on polycrystalline gold: studies using a ferrocenylalkylthiol probe, Langmuir 23 (2007) 292–296.
[38] C.R. Dawson, J.M. Nelson, The influence of catechol on the stability of *o*-benzoquinone in aqueous solutions, J. Am. Chem. Soc. 60 (1938) 245–249.
[39] L. Su, L.Q. Mao, Gold nanoparticle/alkanedithiol conductive films self-assembled onto gold electrode: electrochemistry and electroanalytical application for voltammetric determination of trace amount of catechol, Talanta 70 (2006) 68–74.
[40] A. Ulman, Formation and structure of self-assembled monolayers, Chem. Rev. 96 (1996) 1533–1554.
[41] J. Strutwolf, C.K. O'Sullivan, Microstructures by selective desorption of self-assembled monolayer from polycrystalline gold electrodes, Electroanalysis 19 (2007) 1467–1475.
[42] T.R. Soreta, J. Strutwolf, C.K. O'Sullivan, Eectrochemical fabrication of nanostructured surfaces for enhanced response, Chem. Phys. Chem. 9 (2008) 920–927.
[43] M. Darder, K. Takada, F. Pariente, E. Lorenzo, H.D. Abruña, Dithiobissuccinimidyl propionate as an anchor for assembling peroxidases at electrodes surfaces and its application in a H_2O_2 biosensor, Anal. Chem. 71 (1999) 5530–5537.
[44] J.H. Fuhrhop, T. Bedurke, M. Gnade, J. Schneider, K. Doblhofer, Hydrophobic gaps of steroid size in a surface monolayer collect 1,2-trans-cyclohexanediol and glucose from bulk water, Langmuir 13 (1997) 455–459.
[45] A. Fragoso, N. Laboria, D. Latta, C.K. O'Sullivan, Electron permeable self-assembled monolayers of dithiolated aromatic scaffolds on gold for biosensor applications, Anal. Chem. 80 (2008) 2556–2563.
[46] O. Chailapakul, R.M. Crooks, Interactions between organized, surface-confined monolayers and liquid-phase probe molecules.4. Synthesis and characterization of nanoporous moleculas assemblies — mechanism of probe penetration, Langmuir 11 (1995) 1329–1340.
[47] J.M. Campina, A. Martins, F. Silva, Selective permeation of a liquid-like self-assembled monolayer of 11-amino-1-undecanethiol on polycrystalline gold by highly charged electroactive probes, J. Phys. Chem., C 111 (2007) 5351–5362.
[48] L.Y.S. Lee, R.B. Lennox, Ferrocenylalkylthiolate labeling of defects in alkylthiol self-assembled monolayers on gold, Phys. Chem. Chem. Phys. 9 (2007) 1013–1020.
[49] M.E. Sandison, N. Anicet, A. Glidle, J.M. Cooper, Optimization of the geometry and porosity of microelectrode arrays for sensor design, Anal. Chem. 74 (2002) 5717–5725.